

Determining Activity Coefficients of SOA from Isothermal Evaporation in a Laboratory Chamber

Xiaoxi Liu, Douglas A. Day, Jordan E. Krechmer, Paul J. Ziemann, and Jose L. Jimenez*

Cite This: *Environ. Sci. Technol. Lett.* 2021, 8, 212–217

Read Online

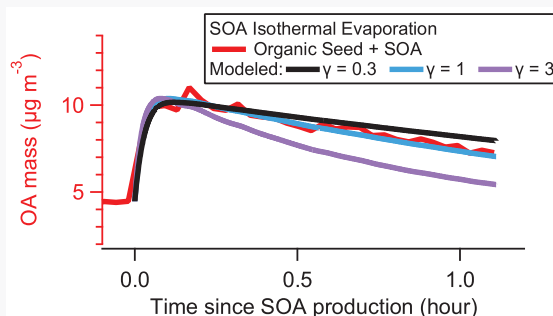
ACCESS |

Metrics & More

Article Recommendations

Supporting Information

ABSTRACT: Nonideal molecular interactions in aerosol particles influence the partitioning of semivolatile organic compounds (SVOCs). However, few direct measurements exist that determine activity coefficients (γ), which quantify nonideality, for individual organic compounds in different atmospheric mixtures. By measuring the isothermal evaporation of SOA formed from multifunctional SVOCs in an environmental chamber, this study determines the mole-fraction-based γ of the bulk SOA in a variety of pre-existing chemically complex particles, approximated as if the bulk SOA behaved like a single SVOC. These multicomponent mixtures contain molecular structures commonly found in the atmosphere. When treated as a single liquid phase, γ of the bulk SOA tends to increase from ~ 1 to ~ 5 as the organic seeds and the SOA have more differing polarities. A high computed γ value of 74 for a wet ammonium sulfate-SOA system indicates phase separation. The γ for some individual species was also quantified based on gas-phase measurements and AIOMFAC model predictions. However, the bulk SOA γ cannot be explained by the simplified speciated SVOC–seed interactions, suggesting incomplete compositional understanding of the bulk SOA. These results demonstrate a method to quantify nonideal behavior and show that it can occur in multicomponent mixtures and therefore influence OA formation, evolution, and lifetimes.



INTRODUCTION

Ambient aerosols consist of complex mixtures of organic and inorganic compounds.¹ The organic fraction is dominated by secondary organic aerosols (SOA), much of which is formed through the gas-to-particle partitioning of low-volatile and semi-volatile organic compounds (L/SVOCs) but also contains primary organic aerosols (POA).^{1–3} In most atmospheric models, organic gas–particle absorptive partitioning is treated as a thermodynamic equilibrium between gas and particle phases.^{4,5} A modified version of the theory states that at equilibrium the fraction of a SVOC in the particle phase depends on its pure compound volatility (c^0), activity coefficient (γ), and total OA mass concentration (c_{OA}).⁶ Here, γ captures the impact of nonideal molecular interactions in aerosol particles, which depend on the interaction of each specific compound with the absorbing aerosol mixture. Nonideal interactions influence organic partitioning, the physical state of the condensed phase, cloud droplet activation, and atmospheric chemistry.^{7,8} In this work, γ has the common meaning of being mole-fraction based with a reference state of $\gamma = 1$ for the pure component at a given temperature and pressure, and $\gamma \leq 1$ favors the particle phase and vice versa. For one liquid phase, γ modifies c^0 to give the effective saturation concentration (c^*) of compound i

$$c_i^* = c_i^0 \gamma_i \frac{\overline{MW}}{MW_i} \quad (1)$$

where \overline{MW} is the mass-fraction-weighted harmonic mean molecular weight of the absorbing phase (Supporting Information), and MW_i is the molecular weight of compound i .^{5,8,9}

The inclusion of activity coefficients in estimating gas–particle partitioning is crucial for accurately predicting aerosol mass concentration and composition. Recent laboratory studies found varying degrees of SOA enhancement and depression depending on the SOA and pre-existing OA compositions.^{10–12} Several approaches have been proposed to explain this variability, such as models that separate multiple liquid phases (e.g., hydrophilic versus hydrophobic phases)^{10,13} and the Hansen solubility framework that predicts miscibility.¹² Still, accurate γ values are needed to quantitatively predict SOA formation.

Due to the complexity of aerosol mixtures, thermodynamic models are valuable for estimating γ in liquid organic, inorganic, and mixed organic–inorganic phases. The Universal Quasi-chemical Functional group Activity Coefficients (UNIFAC)

Received: November 15, 2020

Revised: December 22, 2020

Accepted: December 23, 2020

Published: December 29, 2020



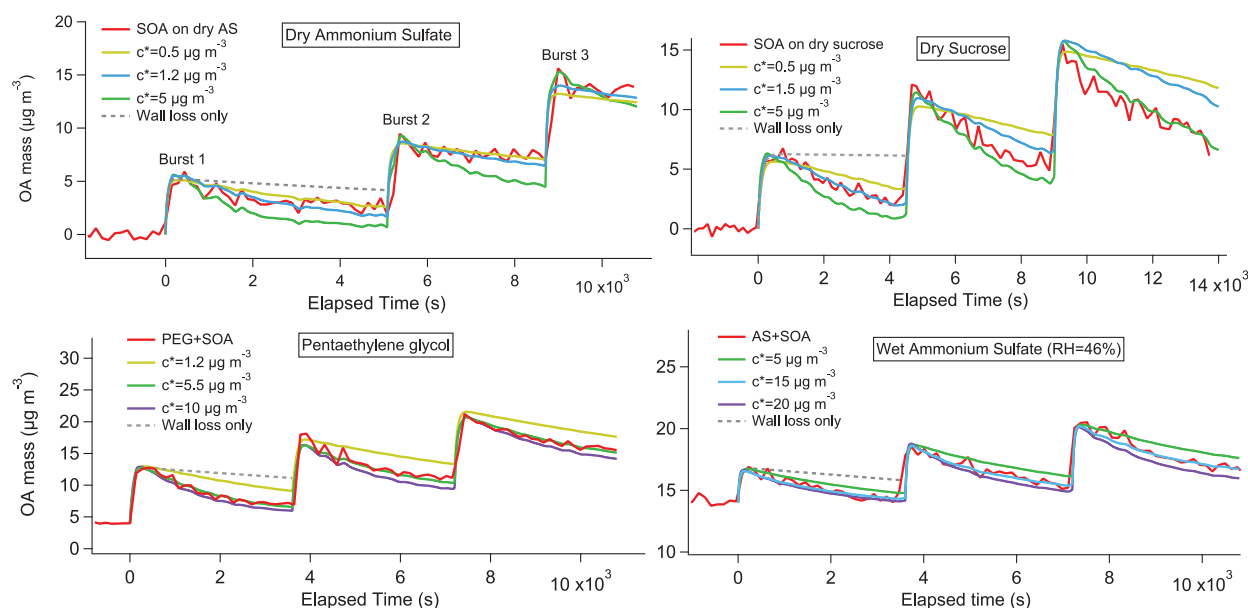


Figure 1. Examples of modeled evaporation using a single effective bulk saturation vapor pressure, together with SMPS measurements. Only the first burst measurements are used to derive the best effective volatility (listed in Table S1), while the following two bursts are also shown using those fitted parameters.

model, based on the group contribution method introduced by Fredenslund et al.,¹⁴ is widely used by the atmospheric aerosol community. On the basis of the UNIFAC approach, many other coupled organic–inorganic models that calculate γ have been developed to improve the organic–inorganic interactions and better represent the atmospherically relevant aerosols.^{15–18} One of them is the Aerosol Inorganic–Organic Mixtures Functional groups Activity Coefficient (AIOMFAC) model, a chemical structure-based model that explicitly incorporates solution nonideality among organics, water, and inorganic ions.^{5,7,15} With proper information about the chemical species involved and environmental conditions, such as in well-characterized laboratory experiments, these models can estimate γ values to compare with measurements.

While water activity in water–organic solutions has been more often measured,^{19,20} experimental quantification of γ of organic compounds relevant to atmospheric aerosol is scarce. Cappa et al.²¹ measured the temperature-dependent evaporation behavior of multicomponent mixtures of dicarboxylic acids and found $\gamma < 1$ for the lower-molecular-weight diacids but $\gamma > 1$ for the heavier diacids. Saleh and Khlystov²² calculated the γ of SVOCs, mainly adipic acid, in several binary solutions by measuring the total change in aerosol volume upon moderate heating. The calculated γ ranged from 0.3 to 3 depending on mixtures and mole fractions. Liu et al.²³ derived c^* of multifunctional SVOCs by fitting their isothermal gas–particle partitioning to observations as measured by mass spectrometry. Variations in c^* of the same SVOC were observed in different seeds, which reflects mainly variability in γ and measurement uncertainties. Further experimental measurements of γ for different aerosol types are important to improve the accuracy of SOA prediction that currently relies more on modeled than measured γ .

This study measures the isothermal evaporation of bulk SOA formed by multifunctional SVOCs in an environmental chamber. Here, we approximate the bulk SOA as having one single volatility, i.e., approximated as if the bulk SOA behaved

like a single SVOC. The mole-fraction-based γ of the bulk SOA in a variety of pre-existing particles of different phases and properties is then derived by fitting the mass concentration evolution to the measurements. These multicomponent mixtures contain molecular structures that are commonly found in the atmosphere and are also diverse. We then explore the trend of γ as the relative polarity of the seeds and the SOA varies. Although the composition of the formed SOA is not fully characterized, we calculate the γ for some known SOA-forming compounds using the c^* values derived in Liu et al.²³ AIOMFAC is also used to predict γ for the same speciated compounds. The comparison among the three sets of γ is discussed.

MATERIALS AND METHODS

The experimental procedures to produce L/SVOCs and measure their gas–particle–wall partitioning in a 20 m³ Teflon environmental chamber is described in detail in Liu et al.²³ and Krechmer et al.²⁴ A brief description is given here. The experimental conditions were maintained at 25 ± 0.3 °C and RH < 1% or RH = 46 ± 1% (humidified using Milli-Q ultrapure water). The pre-existing seeds that provided condensation surfaces and formed mixtures with newly condensed SOA were liquid organics, including oleic acid, squalane, pentaethylene glycol, and dioctyl sebacate (DOS); solid seeds, including ammonium sulfate (AS) and sucrose; liquid inorganic, deliquesced AS; and α -pinene/O₃ SOA that is a realistic atmospheric SOA mixture (Table S1). The volume size distributions in these experiments are typical of tropospheric particles (peaked between 100 and 200 nm). The observed condensing L/SVOCs were produced in the gas phase by a fast (10 s) OH oxidation of a mixture of 1-alkanols (>99% purity, Sigma-Aldrich) under high NO. Well-characterized products in the gas phase of this reaction were measured by nitrate-adduct chemical ionization mass spectrometry (NO₃–CIMS), including dihydroxynitrates (DHNs), trihydroxynitrates (THNs), and carbonyl dihydroxynitrates (CDHNs) (Table S2). The gaseous products were then taken up by particles, producing SOA that

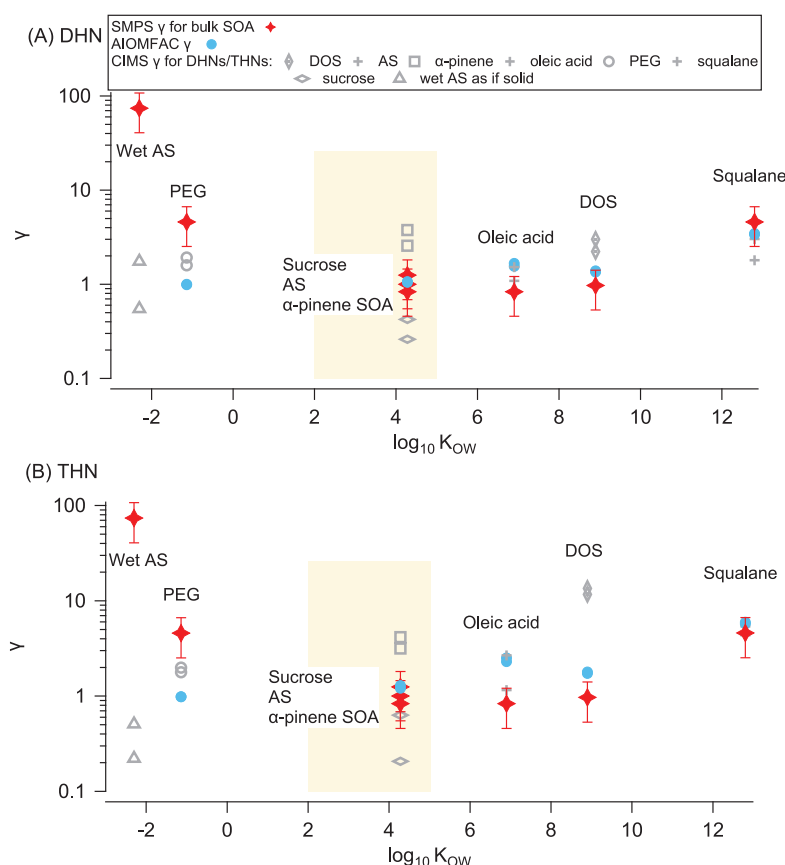


Figure 2. Inferred γ (from SMPS and CIMS measurements) versus n -octanol/water partition coefficient (K_{OW}) of each seed. SMPS measurements are the same in both panels, while CIMS measurements ($\pm 49\%$, not plotted) show DHN (top) and THN (bottom). Shaded area shows K_{OW} for CIMS-measured C_9 – C_{12} DHNs (SIMPOL-estimated $c^0 = 0.8$ – $15 \mu\text{g m}^{-3}$). Also shown are modeled γ using AIOMFAC assuming the OA mixture contains single C_{10} and C_{12} DHN or THN and a corresponding seed, with mass fraction ratios listed in Table S1.

peaked within 2–3 min after the reaction. Offline mass spectrometry showed that the major SOA products are DHNs, with a minor contribution from cyclic hydroxyhemiacetals.^{23,25–27} As the L/SVOCs repartitioned into the gas phase, they were also lost to chamber walls at a slower time scales (~ 17 min). The net effect of this “wall denuding” is a constantly decreasing aerosol volume with time (even when corrected for particle–wall losses), as SVOCs evaporated from the particles to re-establish gas–particle equilibrium. After ~ 1 h, the oxidation burst was usually repeated another 1–2 times. An illustration of SVOC concentration changes in three phases (gas, particle, and wall) since the photochemical reaction is shown in Figure S1.

The size distribution and number concentration of seeds and SOA were measured by a Scanning Mobility Particle Sizer (SMPS) consisting of an electrostatic classifier (TSI, 3080), differential mobility analyzer (TSI, 3081), and a Condensation Particle Counter (TSI, 3775). The SMPS was placed inside the chamber enclosure and was operated under the same temperature and humidity as in the chamber so as not to alter partitioning states or water content.²³ The evaporation of the SOA due to the “wall denuding” effect was captured by the SMPS with a time resolution of 135–145 s.

A box model that includes the condensation and evaporation of oxidized products to and from particles and chamber walls was used to simulate the overall evaporation of bulk SOA (Supporting Information).²³ By fitting the simulated bulk SOA concentration to the SMPS measurements, we determined the

best, well-constrained c^* and total SOA-forming SVOC production for each seeded experiment after the first burst.

For solid seeds, AS and sucrose in our case, the condensed SVOCs are expected to form a layer on the surface of the seed cores so that the SVOCs dissolve in themselves²⁸ (Supporting Information). The activity coefficient γ should equal to 1 in these ideal mixtures, assuming these SVOCs are similar enough to mix ideally. Therefore, we selected c^* in the SOA–AS mixture as the reference and estimated γ for all other seeds, by combining with Equation 1 as

$$\frac{c_{\text{seeded}}^*}{c_{\text{AS}}^*} = \frac{MW_{\text{SOA}}}{MW_{\text{seeded}}}$$

i.e., c^* of a seeded experiment versus that of the AS-seeded experiment and then adjusted by the molecular weight ratio of the seeded experiment. We estimated the 2σ uncertainty of γ to be $\pm 45\%$ (Supporting Information).

RESULTS AND DISCUSSION

We first present results of measured and simulated bulk SOA evaporation. Figure 1 shows four experiments, while the rest are shown in Figure S2. In the four examples, the SOA formation peaked quickly after the 10 s oxidation, then decreased in darkness due to vapor uptake by chamber walls and the resulting particle SOA evaporation. If the SOA was lost only due to particle–wall loss, assuming at a same rate as the measured

decay of the seed volume concentration before photooxidation, the observed SOA decrease would be substantially slower (dashed lines in Figure 1 and Figure S2). Evaporation time series predicted by the model using the best c^* and several other volatilities are also shown. In the c^* sensitivity tests, the total SVOC production was chosen to match the observed SOA peak. Values of best c^* and total SVOC production are listed in Table S1.

Since the interactions between the pre-existing seeds and the produced SVOCs change with the seed properties, we expect that the amount of and/or the types of SVOCs that participate in the gas–particle partitioning are different across the seeds used. The variations in the fitted total SVOC production in Table S1 are consistent with this expectation. The bulk SOA formed might thus have some differences in composition, which is a caveat of this method. However, for almost all seed types, OA composition was measured using an aerosol mass spectrometer (AMS).^{29,30} The SOA mass spectra of all available experiments showed consistent composition.²³

The γ values derived are summarized in Figure 2 and Table S1, plotted versus the seed *n*-octanol/water partition coefficient (K_{OW})³¹ as an indicator of seed polarity. Among the tested seeds, α -pinene/O₃ SOA and oleic acid resulted in the lowest $\gamma = 0.83$, likely indicating that their presence favored vapor condensation. Note that α -pinene/O₃ SOA was treated as a liquid despite being viscous.²³ The second lowest $\gamma = 0.97$ was from the DOS experiment. SOA on top of sucrose was associated with $\gamma = 1.3$, and the deviation from unity can be explained by the experimental uncertainty. Here, γ for squalane and pentaethylene glycol experiments are both 4.6, indicating dissimilarity between the condensing vapors and the aerosol mixture. The deliquesced AS–SOA experiment yielded the highest SOA $\gamma = 74$ and was associated with the least amount of SVOCs forming the observed SOA (Table S1), showing significant deviation from ideality in this solution. This high γ was derived by treating the mixture as a single liquid phase, which is likely inappropriate as Donahue et al.³² found that the boundary for phase separation to occur is near $\gamma \sim 5$ –10. In addition, separation of electrolyte-rich and organic-rich phases is often observed.^{33,34} So an additional model run was performed assuming two separate phases, which yielded a reasonable γ of 1 for the SOA phase (Table S1). For all other organic-seeded experiments, phase separation is less likely as indicated by smaller γ values less than 5 and structural similarities between SVOCs (both carbon chain and polar functional groups) and organic seeds.

The relationship of γ versus the polarity similarity between the seeds and the SOA was then explored. Here, the partition coefficient $\log K_{OW}$ (base 10) was used to characterize the lipophilicity/hydrophilicity (\sim polarity) of each seed and some major SOA-forming compounds, C₆–C₁₂ DHNs and THNs ($c^0 = 0.0056$ – $246 \mu\text{g m}^{-3}$).²⁵ The $\log K_{OW}$ values were calculated by the Discovery Studio software (version 3.0).³¹ In Figure 2, the $\log K_{OW}$ of the seeds increases from left to right. The general trend of γ versus $\log K_{OW}$ is consistent for the bulk results. For seeds with $\log K_{OW}$ closer to those of the partitioning SVOCs, we observe $\gamma \sim 1$. As the seeds become ~ 5 orders of magnitude more hydrophobic (squalane) or more hydrophilic (pentaethylene glycol and wet AS) as quantified by K_{OW} , higher γ values are observed, indicating that these seeds are less hospitable to the condensing vapors.

Using the c^* of DHNs and THNs inferred from the gas-phase CIMS measurements in Liu et al.²³ and Krechmer et al.,²⁴ we

derived their γ relative to the AS case. The CIMS-inferred γ has an estimated uncertainty of $\sim 49\%$, determined similarly as for SMPS-derived γ . In addition, wet AS seed was treated as a separate, nonabsorbing phase (similarly to solid dry AS). Also plotted in Figure 2 are the γ values of C₁₀ and C₁₂ DHNs and THNs, which are the least volatile of the studied SVOC. Those of all other DHNs and THNs are shown in Figure S3. For the DHNs and THNs, the AIOMFAC model was used to predict their γ in a simplified binary solution of the specific species plus the seed, as the detailed composition of the real mixture is unknown. Since AIOMFAC prediction can be sensitive to the mass fractions of input compounds, we used the measured SOA:seed ratios (Table S1) to represent the DHN (or THN):seed mass ratios in the simplified binary solution. The deliquesced AS experiment is excluded from AIOMFAC prediction since the interaction between the organic nitrate group and inorganic ions is not established in the model.¹⁵ For the same type of compounds, i.e., DHNs or THNs in our case, the AIOMFAC-predicted γ varies slightly with the carbon number (Figure S3). For example, if the seed is more hydrophobic, the AIOMFAC γ decreases as the carbon number increases, as expected in a simplified binary solution. When averaged, predicted γ from the AIOMFAC model showed some correlation with the bulk SOA results ($R^2 = 0.26$, Figure S4). Compared to the AIOMFAC method, the single compounds' γ values estimated by CIMS generally differ by factors of 1–5, with THNs in the DOS seed showing the largest differences. In addition, the CIMS-inferred γ showed larger differences than the carbon number can explain. The differences may be due to AIOMFAC simplifications and related uncertainties, uncertainties in the SOA composition used as AIOMFAC input, and experimental uncertainties in the CIMS-based estimates. Compared with the bulk SOA, the dependence of γ of the single compounds (Figure 2 and Figure S3) or their averages (Figure S4) on seed polarity is less obvious, suggesting more complex interactions between DHNs or THNs and seed–SOA mixtures.

The effects of γ values on SOA formation are briefly demonstrated by modeling SOA evolution using $\gamma = 1$ and 5, respectively, as shown in Figure S5. Under typical experimental conditions, the peak SOA formed shortly after photo-oxidation decreased by 25% as γ changed from 1 to 5. In addition, the difference in SOA amounts can persist for hours until all SVOCs (gaseous and particulate) were lost to the chamber walls. Consistent with that result, when considering all seeded experiments studied, a general anticorrelation was seen between the SMPS-inferred, bulk γ versus peak SOA volume produced (Figure S6). As the seed–SOA similarity varied, the measured peak SOA differed by a factor of ~ 3 . Note that the γ values in this study were obtained mostly under dry conditions, and further study is required for humid situations applicable to the lower atmosphere.

In this work, we demonstrated in a chamber an experimental technique to derive the activity coefficients of organic compounds (bulk or speciated) by measuring their volatility-dependent partitioning under atmospherically relevant conditions. The experiments were designed to separate gas–wall and gas–particle partitioning processes based on their different time scales. This technique can be applied to other real atmospheric aerosol systems that contain multifunctional, unstable components that may not be possible to synthesize or isolate or when model calculation is not possible due to lack of knowledge of the mixture composition. This method can also

help constrain functional groups, such as organonitrate, that have high uncertainties in AIOMFAC model parametrization. Reduction of the experimental uncertainties is needed to improve the information obtained from this new method.

The inferred γ of bulk SOA spanned from near 1 to 5 for a variety of organic seeds and a value of 74 indicated phase separation for a wet AS–SOA system. By relating γ with seed polarity (lipophilicity/hydrophilicity), we found that when seed and SOA have more similar polarity, SVOC partitioning increases. The observed nonideality can occur in multi-component mixtures in both the laboratory and atmosphere and therefore influence SOA formation.

■ ASSOCIATED CONTENT

SI Supporting Information

The Supporting Information is available free of charge at <https://pubs.acs.org/doi/10.1021/acs.estlett.0c00888>.

Calculation of mass-fraction-weighted harmonic mean molecular weight, modeling c^* and total SVOC production, determination of γ uncertainty, two-phase versus one-phase assumption for sucrose and SOA mixture, summary of chamber experiments (Table S1), SVOC products (Table S2), illustration of SVOC concentration changes in all three phases (Figure S1), modeled evaporation (Figure S2), inferred γ values and their scatter plots (Figures S3 and S4), modeled effects of γ on SOA production and evolution (Figure S5), bulk SOA γ versus SOA production (Figure S6), and modeled SOA using two volatility bins (Figure S7) (PDF)

■ AUTHOR INFORMATION

Corresponding Author

Jose L. Jimenez – Cooperative Institute for Research in Environmental Sciences (CIRES) and Department of Chemistry, University of Colorado Boulder, Boulder, Colorado 80309, United States; orcid.org/0000-0001-6203-1847; Email: jose.jimenez@colorado.edu

Authors

Xiaoxi Liu – Cooperative Institute for Research in Environmental Sciences (CIRES) and Department of Chemistry, University of Colorado Boulder, Boulder, Colorado 80309, United States; orcid.org/0000-0002-5104-8886

Douglas A. Day – Cooperative Institute for Research in Environmental Sciences (CIRES) and Department of Chemistry, University of Colorado Boulder, Boulder, Colorado 80309, United States; orcid.org/0000-0003-3213-4233

Jordan E. Krechmer – Cooperative Institute for Research in Environmental Sciences (CIRES) and Department of Chemistry, University of Colorado Boulder, Boulder, Colorado 80309, United States; orcid.org/0000-0003-3642-0659

Paul J. Ziemann – Cooperative Institute for Research in Environmental Sciences (CIRES) and Department of Chemistry, University of Colorado Boulder, Boulder, Colorado 80309, United States; orcid.org/0000-0001-7419-0044

Complete contact information is available at:

<https://pubs.acs.org/doi/10.1021/acs.estlett.0c00888>

Author Contributions

X.L., J.E.K., J.L.J., P.J.Z., and D.A.D. designed the experiments. X.L. and J.E.K. conducted experiments and analyzed data. X.L.

led the analyses and wrote the manuscript. All authors provided input in finalizing and revising the manuscript.

Notes

The authors declare no competing financial interest.

■ ACKNOWLEDGMENTS

This work was supported by DOE (BER/ASR) Grant DE-SC0016559, NSF AGS-1822664, and by a CIRES IRP grant. We thank Zhe Peng for discussion and support about the KinSim simulator.

■ REFERENCES

- (1) Jimenez, J. L.; Canagaratna, M. R.; Donahue, N. M.; Prevot, A. S.; Zhang, Q.; Kroll, J. H.; DeCarlo, P. F.; Allan, J. D.; Coe, H.; Ng, N. L.; Aiken, A. C.; Docherty, K. S.; Ulbrich, I. M.; Grieshop, A. P.; Robinson, A. L.; Duplissy, J.; Smith, J. D.; Wilson, K. R.; Lanz, V. A.; Hueglin, C.; et al. Evolution of organic aerosols in the atmosphere. *Science* **2009**, *326* (5959), 1525–1529.
- (2) Robinson, A. L.; Donahue, N. M.; Shrivastava, M. K.; Weitkamp, E. A.; Sage, A. M.; Grieshop, A. P.; Lane, T. E.; Pierce, J. R.; Pandis, S. N. Rethinking Organic Aerosols: Semivolatile Emissions and Photochemical Aging. *Science* **2007**, *315* (5816), 1259–1262.
- (3) Ziemann, P. J.; Atkinson, R. Kinetics, products, and mechanisms of secondary organic aerosol formation. *Chem. Soc. Rev.* **2012**, *41* (19), 6582–605.
- (4) Pankow, J. F. An absorption model of the gas/aerosol partitioning involved in the formation of secondary organic aerosol. *Atmos. Environ.* **1994**, *28* (2), 189–193.
- (5) Zuend, A.; Seinfeld, J. H. Modeling the gas-particle partitioning of secondary organic aerosol: the importance of liquid-liquid phase separation. *Atmos. Chem. Phys.* **2012**, *12* (9), 3857–3882.
- (6) Donahue, N. M.; Robinson, A. L.; Stanier, C. O.; Pandis, S. N. Coupled Partitioning, Dilution, and Chemical Aging of Semivolatile Organics. *Environ. Sci. Technol.* **2006**, *40* (8), 2635–2643.
- (7) Zuend, A.; Marcolli, C.; Peter, T.; Seinfeld, J. H. Computation of liquid-liquid equilibria and phase stabilities: implications for RH-dependent gas/particle partitioning of organic-inorganic aerosols. *Atmos. Chem. Phys.* **2010**, *10* (16), 7795–7820.
- (8) Gorkowski, K.; Preston, T. C.; Zuend, A. Relative-humidity-dependent organic aerosol thermodynamics via an efficient reduced-complexity model. *Atmos. Chem. Phys.* **2019**, *19* (21), 13383–13407.
- (9) Pye, H. O. T.; Zuend, A.; Fry, J. L.; Isaacman-VanWertz, G.; Capps, S. L.; Appel, K. W.; Foroutan, H.; Xu, L.; Ng, N. L.; Goldstein, A. H. Coupling of organic and inorganic aerosol systems and the effect on gas-particle partitioning in the southeastern US. *Atmos. Chem. Phys.* **2018**, *18* (1), 357–370.
- (10) Song, C.; Zaveri, R. A.; Shilling, J. E.; Alexander, M. L.; Newburn, M. Effect of hydrophilic organic seed aerosols on secondary organic aerosol formation from ozonolysis of alpha-pinene. *Environ. Sci. Technol.* **2011**, *45* (17), 7323–9.
- (11) Ye, J.; Gordon, C. A.; Chan, A. W. H. Enhancement in Secondary Organic Aerosol Formation in the Presence of Preexisting Organic Particle. *Environ. Sci. Technol.* **2016**, *50* (7), 3572–3579.
- (12) Ye, J.; Van Rooy, P.; Adam, C. H.; Jeong, C.-H.; Urch, B.; Cocker, D. R.; Evans, G. J.; Chan, A. W. H. Predicting Secondary Organic Aerosol Enhancement in the Presence of Atmospherically Relevant Organic Particles. *ACS Earth Space Chem.* **2018**, *2* (10), 1035–1046.
- (13) Griffin, R. J.; Nguyen, K.; Dabdub, D.; Seinfeld, J. H. A Coupled Hydrophobic-Hydrophilic Model for Predicting Secondary Organic Aerosol Formation. *J. Atmos. Chem.* **2003**, *44* (2), 171–190.
- (14) Fredenslund, A.; Jones, R. L.; Prausnitz, J. M. Group-contribution estimation of activity coefficients in nonideal liquid mixtures. *AIChE J.* **1975**, *21* (6), 1086–1099.
- (15) Zuend, A.; Marcolli, C.; Booth, A. M.; Lienhard, D. M.; Soonsin, V.; Krieger, U. K.; Topping, D. O.; McFiggans, G.; Peter, T.; Seinfeld, J. H. New and extended parameterization of the thermodynamic model AIOMFAC: calculation of activity coefficients for organic-inorganic

mixtures containing carboxyl, hydroxyl, carbonyl, ether, ester, alkenyl, alkyl, and aromatic functional groups. *Atmos. Chem. Phys.* **2011**, *11* (17), 9155–9206.

(16) Ming, Y.; Russell, L. M. Thermodynamic equilibrium of organic-electrolyte mixtures in aerosol particles. *AIChE J.* **2002**, *48* (6), 1331–1348.

(17) Erdakos, G. B.; Chang, E. I.; Pankow, J. F.; Seinfeld, J. H. Prediction of activity coefficients in liquid aerosol particles containing organic compounds, dissolved inorganic salts, and water—Part 3: Organic compounds, water, and ionic constituents by consideration of short-, mid-, and long-range effects using X-UNIFAC.3. *Atmos. Environ.* **2006**, *40* (33), 6437–6452.

(18) Raatikainen, T.; Laaksonen, A. Application of several activity coefficient models to water-organic-electrolyte aerosols of atmospheric interest. *Atmos. Chem. Phys.* **2005**, *5* (9), 2475–2495.

(19) Peng, C.; Chan, M. N.; Chan, C. K. The Hygroscopic Properties of Dicarboxylic and Multifunctional Acids: Measurements and UNIFAC Predictions. *Environ. Sci. Technol.* **2001**, *35* (22), 4495–4501.

(20) Moore, R. H.; Raymond, T. M. HTDMA analysis of multicomponent dicarboxylic acid aerosols with comparison to UNIFAC and ZSR. *J. Geophys. Res.* **2008**, *113* (D4), na DOI: 10.1029/2007JD008660.

(21) Cappa, C. D.; Lovejoy, E. R.; Ravishankara, A. R. Evidence for liquid-like and nonideal behavior of a mixture of organic aerosol components. *Proc. Natl. Acad. Sci. U. S. A.* **2008**, *105* (48), 18687.

(22) Saleh, R.; Khlystov, A. Determination of Activity Coefficients of Semi-Volatile Organic Aerosols Using the Integrated Volume Method. *Aerosol Sci. Technol.* **2009**, *43* (8), 838–846.

(23) Liu, X.; Day, D. A.; Krechmer, J. E.; Brown, W.; Peng, Z.; Ziemann, P. J.; Jimenez, J. L. Direct measurements of semi-volatile organic compound dynamics show near-unity mass accommodation coefficients for diverse aerosols. *Commun. Chem.* **2019**, *2* (1), 98.

(24) Krechmer, J. E.; Day, D. A.; Ziemann, P. J.; Jimenez, J. L. Direct Measurements of Gas/Particle Partitioning and Mass Accommodation Coefficients in Environmental Chambers. *Environ. Sci. Technol.* **2017**, *51* (20), 11867–11875.

(25) Krechmer, J. E.; Pagonis, D.; Ziemann, P. J.; Jimenez, J. L. Quantification of Gas-Wall Partitioning in Teflon Environmental Chambers Using Rapid Bursts of Low-Volatility Oxidized Species Generated in Situ. *Environ. Sci. Technol.* **2016**, *50* (11), 5757–5765.

(26) Algrim, L. B.; Ziemann, P. J. Effect of the Keto Group on Yields and Composition of Organic Aerosol Formed from OH Radical-Initiated Reactions of Ketones in the Presence of NO_x. *J. Phys. Chem. A* **2016**, *120* (35), 6978–6989.

(27) Lim, Y. B.; Ziemann, P. J. Chemistry of Secondary Organic Aerosol Formation from OH Radical-Initiated Reactions of Linear, Branched, and Cyclic Alkanes in the Presence of NO_x. *Aerosol Sci. Technol.* **2009**, *43* (6), 604–619.

(28) You, Y.; Smith, M. L.; Song, M.; Martin, S. T.; Bertram, A. K. Liquid–liquid phase separation in atmospherically relevant particles consisting of organic species and inorganic salts. *Int. Rev. Phys. Chem.* **2014**, *33* (1), 43–77.

(29) Canagaratna, M. R.; Jayne, J. T.; Jimenez, J. L.; Allan, J. D.; Alfarra, M. R.; Zhang, Q.; Onasch, T. B.; Drewnick, F.; Coe, H.; Middlebrook, A.; Delia, A.; Williams, L. R.; Trimborn, A. M.; Northway, M. J.; DeCarlo, P. F.; Kolb, C. E.; Davidovits, P.; Worsnop, D. R. Chemical and microphysical characterization of ambient aerosols with the aerodyne aerosol mass spectrometer. *Mass Spectrom. Rev.* **2007**, *26* (2), 185–222.

(30) DeCarlo, P. F.; Kimmel, J. R.; Trimborn, A.; Northway, M. J.; Jayne, J. T.; Aiken, A. C.; Gonin, M.; Fuhrer, K.; Horvath, T.; Docherty, K. S.; Worsnop, D. R.; Jimenez, J. L. Field-Deployable, High-Resolution, Time-of-Flight Aerosol Mass Spectrometer. *Anal. Chem.* **2006**, *78* (24), 8281–8289.

(31) Ghose, A. K.; Viswanadhan, V. N.; Wendoloski, J. J. Prediction of Hydrophobic (Lipophilic) Properties of Small Organic Molecules Using Fragmental Methods: An Analysis of ALOGP and CLOGP Methods. *J. Phys. Chem. A* **1998**, *102* (21), 3762–3772.

(32) Donahue, N. M.; Epstein, S. A.; Pandis, S. N.; Robinson, A. L. A two-dimensional volatility basis set: 1. organic-aerosol mixing thermodynamics. *Atmos. Chem. Phys.* **2011**, *11* (7), 3303–3318.

(33) Gorkowski, K.; Donahue, N. M.; Sullivan, R. C. Aerosol Optical Tweezers Constrain the Morphology Evolution of Liquid-Liquid Phase-Separated Atmospheric Particles. *Chem.* **2020**, *6* (1), 204–220.

(34) You, Y.; Renbaum-Wolff, L.; Bertram, A. K. Liquid–liquid phase separation in particles containing organics mixed with ammonium sulfate, ammonium bisulfate, ammonium nitrate or sodium chloride. *Atmos. Chem. Phys.* **2013**, *13* (23), 11723–11734.

(35) Pankow, J. F.; Asher, W. E. SIMPOL.1: a simple group contribution method for predicting vapor pressures and enthalpies of vaporization of multifunctional organic compounds. *Atmos. Chem. Phys.* **2008**, *8* (10), 2773–2796.